Title

Experiments Optimized for Magic Angle Spinning and Oriented Sample Solid-State NMR of Proteins

Journal

The Journal of Physical Chemistry B, 117(41)

ISSN

1520-6106

Authors

Das, Bibhuti B
Lin, Eugene C
Opella, Stanley J

Publication Date

2013-10-17

DOI

10.1021/jp407154h

Peer reviewed

Published in final edited form as:
J Phys Chem B. 2013 October 17; 117(41): . doi:10.1021/jp407154h.

Experiments Optimized for Magic Angle Spinning and Oriented Sample Solid-State NMR of Proteins

Bibhuti B. Das, **Eugene C. Lin**, and **Stanley J. Opella***
University of California, San Diego, 9500 Gilman Drive 0307, La Jolla, CA 92093-0307

Abstract

Structure determination by solid-state NMR of proteins is rapidly advancing as result of recent developments of samples, experimental methods, and calculations. There are a number of different solid-state NMR approaches that utilize stationary, aligned samples or magic angle spinning of unoriented 'powder' samples, and depending on the sample and the experimental method can emphasize the measurement of distances or angles, ideally both, as sources of structural constraints. Multi-dimensional correlation spectroscopy of low-gamma nuclei such as ^{15}N and ^{13}C is an important step for making resonance assignments and measurements of angular restraints in membrane proteins. However, the efficiency of coherence transfer predominantly depends upon the strength of dipole-dipole interaction, and this can vary from site to site and between sample alignments, for example, during the mixing of ^{13}C and ^{15}N magnetization in stationary aligned and in magic angle spinning samples. Here, we demonstrate that the efficiency of polarization transfer can be improved by using adiabatic demagnetization and remagnetization techniques on stationary aligned samples; and proton assisted insensitive nuclei cross-polarization in magic angle sample spinning samples. Adiabatic cross-polarization technique provides an alternative mechanism for spin-diffusion experiments correlating ^{15}N/^{15}N and ^{15}N/^{13}C chemical shifts over large distances. Improved efficiency in cross-polarization with 40% – 100% sensitivity enhancements are observed in proteins and single crystals, respectively. We describe solid-state NMR experimental techniques that are optimal for membrane proteins in liquid crystalline phospholipid bilayers under physiological conditions. The techniques are illustrated with data from both single crystals of peptides and of membrane proteins in phospholipid bilayers.

Keywords

membrane proteins; phospholipid bilayers; adiabatic methods; spin-exchange; spin-diffusion; separated local field spectroscopy; structure determination

Introduction

Because membrane proteins reside in the chemically and dynamically heterogeneous liquid crystalline environment of phospholipid bilayers rather than a uniform environment, such as those of aqueous solutions or crystals, they require NMR experiments that take their unique properties into account. Notably, in "…-the so-called physiological state."[1], membrane proteins undergo fast rotation about the bilayer normal and lateral diffusion in the plane of the bilayer, although they are immobilized on NMR timescales ($<10^4$ Hz) in other dimensions[2–4]. Taken together these limited, but rapid motions give membrane proteins mostly 'solid-like' spectroscopic characteristics; for example, their ^{1}H NMR spectra are very broad and barely detectable.

*Corresponding Author: sopella@ucsd.edu, (858) 822-4820.

Samples that consist of protein-containing phospholipid bilayers (proteoliposomes) under physiological conditions of temperature and pH provide near-native conditions for the study of functional membrane proteins. This is generally not possible with competing methods. NMR methods optimized for studies of membrane proteins in liquid crystalline phospholipid bilayers are described in this article, which is complementary to our recent reviews on related topics that relied on earlier versions of these methods[5, 6].

Separated local field (SLF)[7–9] and homonuclear spin-exchange[10–12] experiments are among the mainstays of solid-state NMR of proteins. Two-dimensional versions of these experiments provide substantial spectroscopic resolution, and they can be readily expanded into three- and higher- dimensional experiments for larger proteins, and the measurement of additional frequencies, splittings, and powder patterns associated with individual sites. SLF experiments provide high spectral resolution due to the different orientational dependencies of the anisotropic heteronuclear dipolar and chemical shift interactions, and the observed frequencies provide measurements of the angles between bonds (and functional groups) and the direction of alignment. Homonuclear spin-exchange experiments provide an alternative approach to spectral resolution and semi-quantitative distance measurements, which, among other advantages, can provide assignments of resonances due to the correlation of resonances from proximate sites.

Oriented sample (OS) solid-state NMR is particularly well suited to the study stationary, uniaxially aligned samples[9], such as membrane proteins in magnetically aligned bicelles[10] or macro discs[12], or mechanically aligned bilayers on glass plates[13]. In OS solid-state NMR the basic SLF and spin-exchange experiments provide up to three orientationally-dependent frequencies for each isotopically labeled site (e.g., ^{1}H-^{15}N dipolar coupling, ^{1}H chemical shift, and ^{15}N chemical shift), and this not only resolves among many of the protein's signals, even in crowded spectral regions, but also yields adequate input for structure calculations in aligned samples. In the past, the majority of experiments have relied on direct ^{15}N-detection, and sensitivity has been a limitation because of ^{15}N's low gyromagnetic ratio; selectively or uniformly ^{15}N labeled samples are essential because of the low natural abundance of the nucleus. Furthermore, while assignment schemes that work well with regular secondary structure, often by taking advantage of spectral patterns resulting from selective isotopic labelling, have been implemented in multiple membrane proteins[5, 6], it has been difficult to develop methods for efficiently assigning resonances in regions of proteins with irregular tertiary structure, such as inter-helical loops or the structured portions of the N- and C- termini.

Despite spectroscopic developments that enable the use of uniformly ^{13}C and ^{15}N labeled proteins, and the detection of nuclei with higher gyromagnetic ratios (and consequently sensitivity), i.e., ^{1}H and ^{13}C, limitations remain for stationary samples due to the network of ^{13}C-^{13}C homonuclear dipolar couplings, which are difficult to decouple without compromising the signal-to-noise ratio during direct ^{13}C-detection. Random dilute labelling enables some experiments[14] because of the statistical isolation of the ^{13}C nuclei, although it requires significant compromises including reduced sensitivity and difficulty in performing homonuclear spin-exchange experiments. Consequently, magic angle spinning (MAS) solid-state NMR methods, which average out anisotropic interactions, including homonuclear ^{13}C-^{13}C dipolar couplings, to first order, and yield effectively isotropic resonances in 'solution-like' NMR spectra[15] play essential roles in NMR experiments on uniformly ^{15}N and ^{13}C labeled proteins. Notably, there are now pulse schemes that can be combined with MAS to selectively recouple the anisotropic interactions averaged out by the mechanical rotation[16], which provides significant flexibility in experimental design.

It has been demonstrated that angular measurements obtained from ^{1}H-^{15}N and ^{1}H-^{13}C dipolar couplings and from ^{15}N and ^{13}C chemical shift anisotropy are equivalent, whether made from unoriented samples in stationary or MAS solid-state experiments based on the angular dependence of the spin-interactions relative to the axis of rotational motion or the direction of alignment magnetically aligned samples using oriented sample (OS) solid-state NMR methods. Initial NMR experiments optimized for both MAS and OS approaches have been described, enabling the measurement of heteronuclear dipolar couplings and chemical shift frequencies as angular restraints for structure calculations[17, 18]. In this article we describe several elaborations of solid-state NMR methodology designed specifically for samples of membrane proteins in liquid crystalline phospholipid bilayers with an emphasis on protein structure determination. The efficacy of adiabatic demagnetization and remagnetization pulse scheme in static OS solid-state NMR is demonstrated on single crystal and membrane protein samples. It is shown that higher efficiency in magnetization transfer among homo and hetero nuclei is achievable using a common dipolar bath. Mixing of magnetization between ^{13}C and ^{15}N nuclei is an essential feature of these pulse schemes that transfers magnetization efficiently even when the strength of dipolar interaction is weak. Pulse schemes for multi-dimensional experiments with the measurement of ^{1}H-^{15}N dipolar couplings are demonstrated for magnetically aligned samples and magic angle spinning of rotationally aligned samples.

Experimental Methods

Sample Preparation

Uniformly ^{15}N labeled Pf1 bacteriophage samples were obtained by following the previously published protocol[19]. The samples for the stationary solid-state NMR experiments were prepared with a protein concentration of ~40 mg/ml. The pH of the sample was adjusted to 8.0 using 5mM sodium borate buffer containing 0.1 mM sodium azide. A 5-mm thin wall glass tube containing ~150 μL of sample was used for all stationary sample experiments. Under these conditions, the bacteriophage particles align with their long axis parallel to the direction of the applied magnetic field.

For magic angle spinning solid-state NMR experiments, the unoriented proteoliposome samples were prepared following the protocols described in previous publications[18]. Pf1 coat proteins were extracted from bacteriophage particles by separating the DNA in a mixed organic solution (50% trifluoroethanol, 0.1% trifluoroacetic acid and 49.9% water). The precipitated DNA was pelleted by centrifugation. The supernatant was subjected to nitrogen gas flow for partial removal of solvent followed by lyophilization. In order to completely remove any residual trifluoroacetic acid, water was added and the lyophilization process was repeated twice. NMR samples were prepared by reconstituting the uniformly ^{13}C, ^{15}N labeled proteins in 1,2-dimyristoyl-sn-glycero-3-phosphocholin (DMPC) lipid bilayers following the previously described[18] methods. ^{15}N labeled or uniform ^{13}C, ^{15}N labeled mercury transporter protein (MerFt) were reconstituted in DMPC liposome vesicles at a lipid to protein ratio 5:1 (w/w) and nearly 30 μL of samples were packed in a 3.2 mm rotor. At this concentration, the two-transmembrane helix protein, MerFt, undergoes rapid rotational motion along the bilayer normal above the gel to liquid crystal phase transition temperature.

NMR experiments

^{15}N detected multi-dimensional experiments on magnetically aligned samples were carried out on a Bruker Avance spectrometer with a ^{1}H resonance frequency of 700.1 MHz. ^{13}C detected experiments were performed on a Varian Inova 500 MHz spectrometer. Both the

spectrometers were equipped with homebuilt 5 mm modified Alderman Grant coil (MAGC) double- and triple-resonance probes[20–22].

For one-dimensional experiments on stationary samples, CP-MOIST[23] was employed for cross-polarization, typically with 50 kHz radio frequency (RF) applied to the ^{1}H and ^{15}N-channels. SPINAL-16 modulation was used for ^{1}H decoupling[24] and continuous wave irradiation was used for either ^{13}C or ^{15}N decoupling. Two-dimensional high resolution separated local field spectra were obtained using either the SAMMY[25] or polarization inversion spin exchange at magic angle (PISEMA)[26] pulse sequences that correlates the ^{15}N chemical shift with the associated ^{1}H-^{15}N dipolar coupling, respectively. 41 kHz RF was used during magic sandwich and cross polarization pulses. ^{15}N detected one-dimensional data in Figure 1 were collected with 2 and 64 scans on single crystal and bicelle samples respectively. Two- and three-dimensional SLF spectra with $^{15}N/^{15}N$ homonuclear correlation were obtained with 8–128 scans for single crystal and bacteriophage samples. 32 real data points with a dwell time of 120 μs and 40 μs were collected for both ^{15}N chemical shift and ^{1}H-^{15}N dipolar frequency evolution periods, respectively. All data were recorded with a 4s recycle delay. The aligned bacteriophage sample temperature was maintained at 0 ^{0}C for optimal resolution[27]. The ^{1}H carrier frequency was set following the optimum results observed for each of the samples of bicelle, single crystal and bacteriophages. During adiabatic cross-polarization, ^{1}H RF was varied from 50 kHz to 1 kHz using an amplitude modulated half-Gaussian shape pulse and ^{15}N magnetization was locked at 12 kHz RF field. Half-Gaussian pulses used for adiabatic demagnetization and remagnetization were optimized to maximum RF amplitude of 20 kHz during mixing. For triple resonance experiments, the ^{13}C carrier frequency was set at 55 ppm; and the ^{15}N carrier frequency was set at 80 ppm. The spectra were acquired with 256 complex points and 40 μs dwell time in the direct dimensions, and 16 scans for signal averaging. 36 complex points were acquired in the indirect dimension with 200 μs dwells. The magnetization was transferred from ^{1}H to ^{15}N with 1 ms CP-MOIST at 50kHz of B_1 field for both channels. 60 kHz SPINAL-16, 30 kHz SPINAL-16, and 50 kHz continuous wave (CW) RF were used for decoupling on ^{1}H, ^{13}C, and ^{15}N channels. Adiabatic passage ^{13}C-^{15}N transfer was made with 20 kHz B_1 field on ^{13}C and ^{15}N channels for 3.9 ms, and adiabatic ^{13}C-^{15}N transfer was made with 25 kHz B_1 field on ^{13}C and ^{15}N channels for 8ms. Amplitude modulated half-Gaussian pulses were used for adiabatic demagnetization and remagnetization.

Magic angle spinning (MAS) experiments were performed on a 750 MHz Bruker Avance spectrometer equipped with a Bruker low-E $^{1}H/^{13}C/^{15}N$ triple-resonance 3.2 mm MAS probe. The spinning rate was controlled to 11.11 kHz ± 2 Hz using a Bruker MAS controller. During ^{13}C detection, 100 kHz RF irradiation was used for ^{1}H decoupling with swept frequency two-pulse phase modulation (SW-TPPM)[28], and 2.5 kHz RF irradiation with WALTZ-16 was used for ^{15}N decoupling. Cross-polarization (CP) from ^{1}H to ^{15}N was optimized using amplitude-modulated RF irradiation (100-50%) applied on the ^{1}H channel; 50 kHz RF irradiation on the ^{1}H and ~27 kHz RF irradiation on the ^{15}N channels were applied during the 1 ms contact time. ^{15}N to ^{13}C polarization transfer was accomplished using either proton-assisted insensitive nuclei CP (PAIN-CP)[29] or by double CP pulse schemes. Double CP was accomplished by transferring magnetization from ^{15}N to ^{13}CA or $^{13}C'$ using spectrally induced filtering in combination with cross-polarization (SPECIFIC-CP)[30]. Adiabatic tangential pulses were applied on the ^{13}C channel. Typical RF irradiations of 27 kHz were applied on the ^{15}N channel and ~16 kHz on the ^{13}C channel for band-selective polarization transfer. SW-TPPM decoupling with 100 kHz RF irradiation was applied during the double CP transfer. 50 kHz, 39 kHz and 55 kHz CW RF were applied on the ^{13}C, ^{15}N and ^{1}H channels for spin locking during PAIN-CP. Sample temperature was calibrated externally using ethylene glycol and water peak in proteoliposome samples. Experiments were carried out at sample temperature between 25–30 ºC.

^{1}H-^{15}N dipolar recoupling experiments were carried out using either polarization inversion time averaged nutation spin exchange at magic angle (PITANSEMA)[31] or symmetry based pulse sequence[32] at 11.111 kHz sample spinning. A nutation frequency of 62.5 kHz at a resonance-offset frequency of 44.2 kHz was used during the frequency switched Lee-Goldburg (LG) cycles. An effective nutation frequency of 76.5 kHz was calculated for Lee-Goldburg (LG) pulses with a dwell time of 13.07 μs. A time modulation of 15.4 μs and 7.7 μs for +LG and −LG period was used to average the nutation to one third. The Hartmann-Hahn match to ^{15}N was accomplished with an RF field match to the first order sidebands. Amplitude modulation on the ^{15}N channel was used at nutation frequencies of 36.5 kHz and 14.3 kHz during the phase alternated LG irradiations. The experimentally determined scaling factor of 0.37 was taken into account in data processing.

Two and three-dimensional experiments with $R18^{7}_{1}$ symmetry based pulse scheme were recorded at a spinning speed of 11.111 kHz. Two consecutive π pulses of 5 μs duration each and phase shifted by 70° and −70° were used in the $R18^{7}_{1}$ pulse scheme[32]. Dipolar frequency measurement with ^{15}N detection was carried out with a dwell time of one rotor period for a total dipolar evolution period of 5 ms, 4s recycle delay and 512 scans. 1.8 and 3.6 ms mixing periods were used for PAIN-CP and SPECIFIC-CP. 10 ms chemical shift evolution under proton irradiation were used to record signals from ^{15}N and ^{13}C nuclei.

The chemical shift frequencies were referenced externally to the adamantane methylene ^{13}C resonance at 38.48 ppm and the ammonium sulfate ^{15}N resonance at 26.8 ppm.

Results

Oriented sample solid-state NMR

An advantage of direct spin manipulations and direct-detection of low γ, dilute nuclei, such as ^{15}N, is that their weak homonuclear dipole-dipole interactions do not require decoupling at any stage of the experiments. However, many experimental procedures, including those that lead to assignments of resonances among proximate nuclei and the semi-quantitative measurement of inter-nuclear distances, are based on spin-exchange among like nuclei, and these are generally inefficient for low γ, dilute nuclei. Several techniques have been proposed to enhance spin-exchange among dilute like-nuclei, e.g., ^{15}N, in applications of correlation spectroscopy. Notably, proton driven spin diffusion (PDSD)[33], cross relaxation driven spin diffusion (CRDSD)[34], and Hartmann-Hahn mismatch mixing (HHMM)[35] schemes have been shown to be useful methods to correlate ^{15}N sites in oriented sample (OS) solid-state NMR. Using these methods, sequential resonance assignments have been made in membrane proteins.[36]. The performance of the above spin diffusion techniques has been compared by Traaseth et al[37]. Additionally, spin diffusion through cross-relaxation via local fields can correlate dilute nuclei, e.g., ^{13}C or ^{15}N that are separated by relatively large distances.

Adiabatic cross-polarization via an intermediate dipolar-ordered state can significantly increase polarization of dilute nuclei compared to conventional cross-polarization (CP) techniques such as Hartmann-Hahn spin-lock matching and through-bond polarization transfer[38]. Adiabatic demagnetization/remagnetization in the rotating frame (ADRF/ARRF) converts the Zeeman order of the abundant nuclei to dipolar order, and then, into Zeeman order of the dilute nuclei for detection. Several adiabatic cross-polarization schemes have been proposed that polarize the dilute nuclei to an extent that is many times greater than possible through direct polarization[38, 39]. It has been shown that CP-ADRF in combination with polarization inversion spin exchange at magic angle (PISEMA[26]) can provide very high sensitivity in two-dimensional SLF experiments[40]. ADRF/ARRF has also been shown to facilitate spin diffusion.[41]

Adiabatic cross-polarization from ^{1}H to ^{15}N in single crystal and aligned protein samples is demonstrated with the spectra in Figure 1. Signals obtained with conventional Hartmann-Hahn cross-polarization under phase alternated pulses, CP-MOIST (cross-polarization mismatch optimized IS transfer)[23], are shown in Figure 1A. CP-MOIST is an alternative to conventional continuous-wave spin-lock cross-polarization under matched Hartmann-Hahn conditions[42] that is more tolerant to RF amplitude mismatch. In practice, CP-MOIST is less tolerant towards ^{1}H irradiation frequency offset and as a result sensitivity is compromised (data not shown here). Moreover, equal or superior performance is observed in CP-ADRF (Figure 1B and D) with low power RF irradiation resulting in less sample heating of electrically lossy samples, such as hydrated membrane proteins in phospholipid bilayers. Reduction in sample heating is essential for maintaining the stability of proteins at high resonance frequencies[20]. Sensitivity enhancement resulting from the use of CP-ADRF is demonstrated by the comparison of intensities in the spectra in Figure 1A and B. In a single crystal, increase in intensities of up to a factor of two can be observed. In membrane proteins sensitivity enhancements in the 20%–40% range are typically observed, reduced from those seen in crystalline compounds largely due to the short relaxation time (T_{1D}) of the dipolar reservoir that is a consequence of the protein's rotational diffusion about the bilayer normal. Nonetheless, the enhancement factor along with low RF sample heating and broad excitation profile are very helpful in the execution of OS solid-state NMR studies of membrane proteins.

The spectra of crystals and proteins in Figure 1 were obtained with initial preparation of ^{1}H transverse magnetization using a hard 90º pulse. Magnetization was then transferred from Zeeman order to dipolar order adiabatically using an amplitude modulated half-Gaussian pulse. The ^{15}N nuclei were polarized with low power continuous wave RF irradiation. It is noteworthy that a simultaneous adiabatic demagnetization pulse applied on ^{1}H and remagnetization pulse on ^{15}N channel can be used to create the polarization for ^{15}N nuclei. The dipolar reservoir can also be used to propagate spin diffusion if contact with the rare spins can be established. Figure 2 contains diagrams for a selection of pulse schemes that utilize adiabatic demagnetization and remagnetization pulses to facilitate spin diffusion among dilute nuclei. Homonuclear correlation spectra with ^{15}N detection were acquired using either of the pulse schemes shown in Figure 2A and B.

In the examples of spectra of a single crystal of ^{15}N-acetyl-leucine (NAL) at an arbitrary orientation and uniformly ^{15}N labeled, magnetically aligned Pf1 bacteriophage in Figure 3, the ^{15}N nuclei were polarized using ADRF prior to chemical shift evolution in the indirect dimension. The SLF spectra in Figure 3A and F show the heteronuclear ^{1}H-^{15}N dipolar couplings associated with the chemical shift frequencies. Figure 3 also contains homonuclear spin-exchange correlation spectra. The single crystal spectra with signals from four unique sites are in the top row and the bacteriophage coat protein spectra with signals from >40 unique amide sites are in the bottom row. Following cross polarization, a flip back 90º pulse was applied to select cosine and sine modulated shift coherences. A z-filter period was used to eliminate any remaining transverse magnetization while preserving the signals of interest. During the mixing period, Zeeman order of the ^{15}N nuclei was transferred to dipolar order using adiabatic demagnetization, spin lock, or adiabatic remagnetization-demagnetization pulses to propagate the dipolar order through $^{1}H/^{1}H$ spin diffusion. The transfer of ^{15}N dipolar order back to Zeeman order was achieved using adiabatic remagnetization. The spin diffusion among ^{1}H can be partially or fully suppressed using almost any homonuclear decoupling pulse scheme, such as Lee-Goldburg[43], or heteronuclear decoupling irradiations[44]. There is no correlation spectrum (only diagonal peaks) observed in the presence of heteronuclear decoupling, which confirms that spin-diffusion occurs via dipolar order. The spectrum in Figure 3H was obtained with ^{1}H decoupling during the mixing period while adiabatic demagnetization-remagnetization of the

dilute ^{15}N nuclei was active. No cross peaks were observed, as expected, since dipolar order cannot be transferred since heteronuclear decoupling removes any contact with the local field reservoir.

PDSD with a 4 sec mixing period results in correlation among the four uniquely oriented ^{15}N sites in the unit cell of the NAL crystal (Figure 3B). However, the transfer of magnetization is relatively weak, which is why the cross-peak intensities are much lower than those of the diagonal signals. In contrast, with adiabatic mixing, uniform polarization transfer occurs among all four signals (Figure 3C). This may result from all of the nuclei being connected to a common dipolar reservoir enabling transfer of dipolar order to Zeeman order to occur equally. ^{15}N/^{15}N shift correlation spectrum for a uniform ^{15}N labeled Pf1 bacteriophage sample is shown in Figure 3G. A number of high intense cross-peaks are easily distinguishable in this two-dimensional spectrum.

The two-dimensional SLF spectrum of the NAL single crystal is shown in Figure 3A. The spectrum was recorded using the high resolution SLF experiment, SAMPI4[25]. The equivalent SLF spectrum obtained for the coat protein in Pf1 bacteriophage particles with adiabatic mixing is quite crowded (Figure 3F). The spectrum was recorded using the pulse scheme shown in Figure 2E in a two-dimensional fashion without ^{15}N shift evolution. The data represent the cross-correlation among dipolar-coupled systems connected to a common dipolar bath. The resolution of the protein spectrum is greatly enhanced in three-dimensional SLF/correlation experiments that result in a correlation of ^{1}H-^{15}N dipolar coupling frequencies and the ^{15}N/^{15}N chemical shift frequencies in three orthogonal dimensions. The pulse scheme shown in Figure 2E was used to obtain the three-dimensional spectra. In this experiment, ^{15}N magnetization was polarized using the CP-MOIST technique prior to spin exchange under frequency switched Lee-Goldburg decoupling. Following the spin exchange period, ^{1}H decoupled ^{15}N chemical shifts were encoded in the first indirect dimension. A 90º flip back pulse was applied to select cosine and sine modulated shift coherences. A z-filter period was used to eliminate any remaining transverse magnetization while preserving the signals of interest. Spin-diffusion between ^{15}N nuclei was carried out under adiabatic demagnetization/remagnetization mixing followed by the direct detection of free chemical shift evolution under proton decoupling. Dipolar evolution during the spin exchange period was encoded in a third dimension. Two-dimensional planes correlating ^{15}N/^{15}N shifts extracted at 5 kHz and 3 kHz ^{1}H-^{15}N dipolar coupling frequencies from the three-dimensional spectrum of the single crystal are shown in Figure 3D and E, respectively. The two-dimensional planes shown in Figure 3I and J were extracted at 9.7 kHz and 6.7 kHz ^{1}H-^{15}N dipolar coupling frequencies, respectively, from the three-dimensional spectrum of the protein. Several resonance assignments are marked following the previously published assignments by Thiriot et al[19, 27].

Uniform ^{13}C labeling plays a crucial role in complete sequential assignments of protein backbones. Hence, heteronuclear correlation of ^{13}C and ^{15}N signals is an essential building block for making resonance assignments. In OS solid state NMR, direct ^{13}C detection improves sensitivity compared to ^{15}N detection. However, it is not practical in all cases because, among other reasons, homonuclear dipolar coupling enhances the relaxation effect due to motions on inconvenient timescales, and therefore broadens the line width resulting in degradation of resolution. The performance of adiabatic pulse schemes is demonstrated on a ^{13}Cα/^{15}N labeled single crystal in Figure 4 with heteronuclear correlation spectra obtained using adiabatic passage and demagnetization/remagnetization techniques.

The spectrum shown in Figure 4A was obtained with adiabatic demagnetization of the ^{15}N nuclei and simultaneous remagnetization of the ^{13}C nuclei. This was carried out using the pulse scheme shown in Figure 2C. Magnetization transfer takes place when both of these

dilute nuclei are connected to the dipolar bath. Nearly half of the magnetization was recovered compared to the use of $^{1}H/^{13}C$ CP-MOIST. Similarly, the $^{13}C\alpha/^{15}N$ correlation spectrum using the adiabatic passage cross polarization scheme during mixing is shown in Figure 4B. It was obtained using the pulse sequence diagrammed in Figure 2D. A tangential pulse was used for ^{13}C during the cross polarization from ^{15}N to ^{13}C. Three out of four molecules in a unit cell have relatively strong $^{13}C\alpha$-^{15}N dipolar couplings, and transfer 80%–90% of the magnetization. However, the signal at 64 ppm is relatively weak due to the fact that $^{13}C\alpha$-^{15}N dipolar coupling at this orientation of the crystal is relatively weak. Polarization transfer via adiabatic passage shows only one bond correlation. Notably, the spectrum in Figure 4A shows uniform polarization transfer among all four molecules in the unit cell, and is an important demonstration that magnetization can be transferred across relatively long molecular distances via dipolar order propagation.

Magic angle spinning solid-state NMR

Magic angle spinning solid-state NMR spectroscopy enables high-resolution spectra to be obtained from unoriented ‘powder’ samples of proteins. However, it has the disadvantage of strongly attenuating the anisotropic properties of the nuclear spin interactions, such as the chemical shift and dipole-dipole couplings between neighbouring nuclei that are relied on for the experiments on stationary samples, as discussed above. Recent developments in decoupling and recoupling pulse schemes suspend the averaging effects of magic angle spinning and retain the geometrical information without sacrificing the high sensitivity and resolution provided by MAS. Heteronuclear dipolar coupling frequencies are recoupled by a wide variety of pulse schemes based on the Hartmann-Hahn match condition under MAS[31, 45, 46]. There are numerous applications that use heteronuclear dipolar coupling measurements to characterize the structure and dynamics of small organic molecules[47] and biomolecules[48, 49]. Symmetry-based pulse sequences are of particular importance in this approach[50]. Applied on one or two channels they can restore the averaging effect on the other nuclei such as ^{13}C and ^{15}N during detection[32, 51]. In particular, ^{1}H-^{15}N dipolar coupling measurements with direct ^{13}C-detection is a crucial development for increasing the sensitivity for applications to proteins and other biomolecules. Symmetry based pulse design offers a broad range of experiments that are applicable to moderate, fast and ultra-fast MAS techniques[18, 32, 52]. In our recent studies of uniformly ^{13}C and ^{15}N labeled proteins, we used symmetry based pulse schemes to measure heteronuclear dipolar frequencies in membrane proteins under MAS[18].

Recently developed pulse sequences[31] are quite efficient in recoupling powder line shapes such as Pake doublets under MAS for uniformly labeled proteins. The measurements are carried out in two ways, either by proton evolved local field[53] or by SLF. PISEMA, originally developed for oriented solid state NMR, can also be applied in MAS experiments with the Hartmann-Hahn match to the first and second sidebands[45]. This provides a maximum theoretical scaling factor of 0.577. Time averaged nutation incorporated into PISEMA (PITANSEMA) under MAS reduces the required RF power on the low γ nuclei[31]. The recoupled spectrum for a ^{1}H-^{15}N dipolar frequency in a uniformly $^{13}C/^{15}N$ labeled NAL crystal is shown in Figure 5C.

A series of symmetry pulses can also be used for recoupling of hetero-nuclear dipolar couplings[32]. $R18^{7}_{1}$ and $R18^{5}_{2}$ pulse schemes are particularly useful under moderate sample spinning speeds. Several other pulse sequences based on the symmetry principle with rotor synchronization have also been reported[52] for ultra-fast spinning speed. $R18^{7}_{1}$ consists of a pair of $180_{70}180_{-70}$ pulse pairs, where each 180° pulse occupies exactly 1/18 of a rotor period. A total of 9 repetitions of pulse pairs are applied over one rotor period and requires RF field strength of 9 times the spinning frequency. However, R18^{7}1 irradiation leads to recoupling of ^{1}H–^{15}N dipolar couplings and ^{1}H chemical shift anisotropy when applied on

the ^{1}H channel. All other interactions notably homo-nuclear dipolar interactions among the ^{1}H spins are suppressed. This provides a theoretical scaling factor of 0.36 for $R18^{7}_{1}$. A two-pulse phase modulation with 70° and −70° phases for each pulse length of 5 μs were used in $R18^{7}_{1}$ cycle under 11.111 kHz spinning. A recoupled dipolar spectrum for a polycrystalline sample of NAL is shown in Figure 5B. Both of the experimental spectra in the Figure were rescaled according to the theoretical scaling factor. As can be seen the symmetry based pulse scheme selectively recouples the perpendicular edge of the Pake doublet with higher efficiency than other orientations in the crystals. SLF experiments in MAS solid-state NMR correlate the isotropic shifts with recoupled dipolar coupling (DC) frequencies, in contrast to OS solid-state NMR, where anisotropic shifts are correlated to heteronuclear DC frequencies.

Two-dimensional ^{13}C or ^{15}N detected SLF experiments that correlate ^{1}H-^{15}N dipolar coupling frequencies with ^{13}C or ^{15}N isotropic chemical shifts are performed in two steps using the pulse scheme shown in Figure 2F. First, ^{13}C or ^{15}N magnetization is generated by cross-polarization from ^{1}H prior to dipolar evolution. Second, ^{1}H-^{15}N dipolar evolution was carried out under $R18^{7}_{1}$ symmetry pulse sequences to assist in the simultaneous recoupling of hetero-nuclear and decoupling of homonuclear dipolar couplings. ^{1}H-^{15}N DC frequencies were encoded in a constant time manner with refocusing of ^{13}C or ^{15}N chemical shifts. The evolution of the isotropic chemical shift frequencies is measured under hetero-nuclear decoupling of ^{1}H in the direct dimension. In a similar fashion, the SLF experiment can be extended to ^{15}N edited ^{13}C detection. This can be achieved by adding a third step to the SLF pulse scheme. After dipolar evolution, ^{15}N magnetization is transferred to either ^{13}Cα or ^{13}C′ using spectrally induced filtering in combination with cross polarization (SPECIFIC-CP)[54]. The ^{13}C signals are enhanced using adiabatic passage cross-polarization from ^{15}N, which is then detected under ^{1}H decoupling. For comparison, two-dimensional ^{15}N detected ^{1}H-^{15}N/^{15}N or ^{15}N edited ^{1}H-^{15}N/^{13}C correlation spectra are shown in Figure 6. Single site resolution for ^{15}N and ^{13}C chemical shifts correlating ^{1}H-^{15}N dipolar frequency in a uniform ^{13}C, ^{15}N labeled NAL polycrystalline sample is shown in Figure 6A, B and E respectively. As expected, similar resolution in dipolar slices but higher sensitivity in case of ^{13}C detection are observed. The two-dimensional SLF spectra with ^{13}C detection were obtained using the pulse scheme shown in Figure 2F and G without the incorporation of ^{15}N shift evolution. Similar experiments were performed on a proteoliposome sample containing a 60-residue two-transmembrane helices mercury transporter protein (MerFt). ^{15}N and ^{13}C detected SLF-2D spectra recorded at 25 ºC are shown in Figure 6C and D respectively. At this temperature the protein undergoes fast rotational diffusion along the bilayer normal[18].

Variations in dipolar frequency that range between 0 kHz to +/− 5 kHz (maximum for the parallel edge of the ^{1}H-^{15}N Pake powder pattern) are observed due to the differential rotational alignment of sites in the membrane proteins along the bilayer normal. A ^{13}C detected SLF spectrum shows better resolution and sensitivity compared to that obtained using ^{15}N detection. A few assigned signals with dipolar and shift frequencies are noted following the previous publication[18]. Adiabatic passage cross-polarization at this temperature showed efficient polarization transfer for strong ^{13}C-^{15}N dipolar coupled spins but relatively weaker signals for small dipolar-coupled spins. This is a practical limitation to rotationally aligned samples where the ^{13}C-^{15}N-dipolar frequencies may vary over a range of 0–1000 Hz. On the other hand, PAIN-CP utilizes a dipolar coupled ^{1}H bath to propagate the dipolar order and transfer magnetization efficiently over long range distances even for spin systems with negligible ^{13}C-^{15}N dipole-dipole interaction[29]. This is demonstrated on a uniform ^{13}C, ^{15}N labeled NAL poly crystals (Figure 6E) and uniformly ^{13}C, ^{15}N labeled Pf1 coat protein in DMPC proteoliposome sample (Figure 7). The 2D-spectrum in Figure 6E correlates ^{1}H-^{15}N dipolar frequency with ^{13}C shifts. Note that all the carbons within the molecule are correlated with uniform intensity. Two-dimensional ^{13}C/^{15}N shift correlation

spectra in Figure 7 were recorded at 25 ºC with adiabatic passage/SPECIFIC CP (Figure 7A) and PAIN-CP (Figure 7B) mixing respectively. Adiabatic mixing shows selective transfer of magnetization to $^{13}C\alpha$ shifts. Where as a number of carbon atoms within the same residue and nearby amino acids are correlated to a single ^{15}N shift with PAIN-CP mixing. This is an important demonstration of distribution of ^{15}N magnetization to distant ^{13}C nuclei with negligible direct dipole-dipole interaction. Henceforth, PAIN-CP may be a method of choice in the study of membrane proteins. Higher resolution is achievable through incorporation of a ^{15}N chemical shift evolution period as the third dimension. The first two-dimensional plane correlating $^{13}C/^{15}N$ shifts in MerFt is shown in Figure 8A. ^{15}N shifts for residues 69, 31 and 14 are marked. Corresponding two-dimensional planes correlating ^{1}H-^{15}N DC/^{13}C shifts at the ^{15}N shift frequencies for D69, L31 and G14 residues are shown in Figure 8B, C, and D, respectively.

Conclusions

Although adiabatic methods have been available since the early days of high resolution solid-state NMR, they provided little in the way of specific advantages for single- and poly-crystalline samples. However, with the growth of solid-state NMR of proteins, their advantages become crucial components of the design and implementation of new experiments. They help deal with limitations imposed by both the dynamics of supramolecular assemblies, for example the rotational diffusion of virus particles and of membrane proteins in phospholipid bilayers, and the fundamental sensitivity limitations of dealing with low γ, dilute nuclei.

The use of adiabatic and other refinements are illustrated here for the two principal classes of solid-state NMR experiments. These are for stationary samples, where the full static dipolar and chemical shift interactions must be dealt with, and for samples undergoing magic angle spinning, where the primary objective is to recover some or all of the same spin interactions that have been averaged out by the sample rotation. Adiabatic cross-polarization method is shown to provide higher sensitivity and tolerance towards a number of experimental errors such as Hartmann-Hahn mismatch, RF inhomogeneity and carrier frequency offsets. It is also shown that adiabatic mixing distributes magnetization efficiently and in a fast order than PDSD scheme (5ms adiabatic mixing period compared to 4s in PDSD). Additionally, correlation spectroscopy is shown for low γ nuclei separated over large distances and negligible dipole-dipole interaction. This is demonstrated in Figure 3 and 4. Figure 4 illustrates the substantial gains in spin-exchange in a stationary sample by invoking adiabatic methods. However, the method may be limited by certain systems with short relaxation time T_{1D} of dipolar bath. The results shown in this article provide an alternative pathway to further development of pulse schemes for sequential assignment in OS using the adiabatic mixing method. The benefits of multi-dimensional experiments that exploit recoupling during magic angle spinning are shown in Figures 6–8. The flexibility in choice of pulse sequences enables physiological conditions of pH and temperature to be used and to avoid the addition of cryoprotectants and other agents needed for low temperature and sensitivity enhancement experiments. In combination these methods increase the feasibility of high-resolution NMR studies of proteins in the variety of situations needed to prepare functionally active samples of proteins in supramolecular assemblies.

Acknowledgments

We thank Chris Grant and Albert Wu for assistance with instrumentation. The research was supported by Grants RO1GM066978 and RO1GM099986 from the National Institutes of Health. It utilized the Biomedical Technology Resource for NMR Molecular Imaging of Proteins at the University of California, San Diego supported by P41EB002031.

References

1. Anfinsen CB. Principles That Govern the Folding of Protein Chains. Science. 1973; 181:223–230. [PubMed: 4124164]
2. Singer SJ, Nicolson GL. The Fluid Mosaic Model of the Structure of Cell Membranes. Science. 1972; 175:720–731. [PubMed: 4333397]
3. Edidin M. Rotational and Translational Diffusion in Membranes. Annu Rev Biophys Bioeng. 1974; 3:179–201. [PubMed: 4371655]
4. Lewis BA, Harbison GS, Herzfeld J, Griffin RG. Nmr Structural Analysis of a Membrane Protein: Bacteriorhodopsin Peptide Backbone Orientation and Motion. Biochemistry. 1985; 24:4671–4679. [PubMed: 4063350]
5. Opella SJ. Structure Determination of Membrane Proteins by Nuclear Magnetic Resonance Spectroscopy. Annu Rev Anal Chem (Palo Alto Calif). 2013; 6:305–328. [PubMed: 23577669]
6. Opella SJ. Structure Determination of Membrane Proteins in Their Native Phospholipid Bilayer Environment by Rotationally Aligned Solid-State Nmr Spectroscopy. Acc Chem Res. 2013
7. Waugh JS. Uncoupling of Local Field Spectra in Nuclear Magnetic Resonance: Determination of Atomic Positions in Solids. Proc Natl Acad Sci U S A. 1976; 73:1394–1397. [PubMed: 1064013]
8. Hester RK, Ackerman JL, Neff BL, Waugh JS. Separated Local Field Spectra in Nmr: Determination of Structure of Solids. Phys Rev Lett. 1976; 36:1081.
9. Opella SJ, Waugh JS. Two-Dimensional 13c Nmr of Highly Oriented Polyethylene. J Chem Phys. 1977; 66:4919–4924.
10. Caravatti P, Deli J, Bodenhausen G, Ernst RR. Direct Evidence of Microscopic Homogeneity in Disordered Solids. J Am Chem Soc. 1982; 104:5506–5507.
11. Szeverenyi NM, Sullivan MJ, Maciel GE. Observation of Spin Exchange by Two-Dimensional Fourier Transform 13c Cross Polarization-Magic-Angle Spinning. J Magn Reson. 1982; 47:462–475.
12. Frey MH, Opella SJ. Carbon-13 Spin Exchange in Amino Acids and Peptides. J Am Chem Soc. 1984; 106:4942–4945.
13. Pake GE. Nuclear Resonance Absorption in Hydrated Crystals: Fine Structure of the Proton Line. J Chem Phys. 1948; 16:327–336.
14. Filipp FV, Sinha N, Jairam L, Bradley J, Opella SJ. Labeling Strategies for 13c-Detected Aligned-Sample Solid-State Nmr of Proteins. J Magn Reson. 2009; 201:121–130. [PubMed: 19781966]
15. Schaefer J, Stejskal EO. Carbon-13 Nuclear Magnetic Resonance of Polymers Spinning at the Magic Angle. J Am Chem Soc. 1976; 98:1031–1032.
16. Chan JCC, Tycko R. Recoupling of Chemical Shift Anisotropies in Solid-State Nmr under High-Speed Magic-Angle Spinning and in Uniformly 13c-Labeled Systems. J Chem Phys. 2003; 118:8378–8389.
17. Park SH, Das BB, De Angelis AA, Scrima M, Opella SJ. Mechanically, Magnetically, and "Rotationally Aligned" Membrane Proteins in Phospholipid Bilayers Give Equivalent Angular Constraints for Nmr Structure Determination. J Phys Chem B. 2010; 114:13995–14003. [PubMed: 20961141]
18. Das BB, Nothnagel HJ, Lu GJ, Son WS, Tian Y, Marassi FM, Opella SJ. Structure Determination of a Membrane Protein in Proteoliposomes. J Am Chem Soc. 2012; 134:2047–2056. [PubMed: 22217388]
19. Thiriot DS, Nevzorov AA, Zagyanskiy L, Wu CH, Opella SJ. Structure of the Coat Protein in Pf1 Bacteriophage Determined by Solid-State Nmr Spectroscopy. J Mol Biol. 2004; 341:869–879. [PubMed: 15288792]
20. Grant CV, Wu CH, Opella SJ. Probes for High Field Solid-State Nmr of Lossy Biological Samples. J Magn Reson. 2010; 204:180–188. [PubMed: 20435493]
21. Grant CV, Yang Y, Glibowicka M, Wu CH, Park SH, Deber CM, Opella SJ. A Modified Alderman-Grant Coil Makes Possible an Efficient Cross-Coil Probe for High Field Solid-State Nmr of Lossy Biological Samples. J Magn Reson. 2009; 201:87–92. [PubMed: 19733108]

22. Lin EC, Wu CH, Yang Y, Grant CV, Opella SJ. 1h-13c Separated Local Field Spectroscopy of Uniformly 13c Labeled Peptides and Proteins. J Magn Reson. 2010; 206:105–111. [PubMed: 20637662]
23. Levitt MH, Suter D, Ernst RR. Spin Dynamics and Thermodynamics in Solid-State Nmr Cross Polarization. J Chem Phys. 1986; 84:4243–4255.
24. Fung BM, Khitrin AK, Ermolaev K. An Improved Broadband Decoupling Sequence for Liquid Crystals and Solids. J Magn Reson. 2000; 142:97–101. [PubMed: 10617439]
25. Nevzorov AA, Opella SJ. A “Magic Sandwich” Pulse Sequence with Reduced Offset Dependence for High-Resolution Separated Local Field Spectroscopy. J Magn Reson. 2003; 164:182–186. [PubMed: 12932472]
26. Wu CH, Ramamoorthy A, Opella SJ. High-Resolution Heteronuclear Dipolar Solid-State Nmr Spectroscopy. J Magn Reson. 1994; A109:270–272.
27. Thiriot DS, Nevzorov AA, Opella SJ. Structural Basis of the Temperature Transition of Pf1 Bacteriophage. Protein Sci. 2005; 14:1064–1070. [PubMed: 15741342]
28. Thakur RS, Kurur ND, Madhu P. Swept-Frequency Two-Pulse Phase Modulation for Heteronuclear Dipolar Decoupling in Solid-State Nmr. Chem Phys Lett. 2006; 426:459–463.
29. Lewandowski JR, De Paëpe G, Griffin RG. Proton Assisted Insensitive Nuclei Cross Polarization. J Am Chem Soc. 2007; 129:728–729. [PubMed: 17243786]
30. Baldus M, Petkova AT, Herzfeld J, Griffin RG. Cross Polarization in the Tilted Frame: Assignment and Spectral Simplification in Heteronuclear Spin Systems. Molecular Physics: An International Journal at the Interface Between Chemistry and Physics. 1998; 95:1197–1207.
31. Yamamoto K, Ermakov VL, Lee DK, Ramamoorthy A. Pitansema-Mas, a Solid-State Nmr Method to Measure Heteronuclear Dipolar Couplings under Mas. Chem Phys Lett. 2005; 408:118–122. [PubMed: 16652173]
32. Zhao X, Edén M, Levitt MH. Recoupling of Heteronuclear Dipolar Interactions in Solid-State Nmr Using Symmetry-Based Pulse Sequences. Chem Phys Lett. 2001; 342:353–361.
33. Suter D, Ernst RR. Spin Diffusion in Resolved Solid-State Nmr Spectra. Phys Rev B: Condens Matter. 1985; 32:5608–5627. [PubMed: 9937807]
34. Xu J, Struppe J, Ramamoorthy A. Two-Dimensional Homonuclear Chemical Shift Correlation Established by the Cross-Relaxation Driven Spin Diffusion in Solids. J Chem Phys. 2008; 128:052308. [PubMed: 18266425]
35. Nevzorov AA. Mismatched Hartmann-Hahn Conditions Cause Proton-Mediated Intermolecular Magnetization Transfer between Dilute Low-Spin Nuclei in Nmr of Static Solids. J Am Chem Soc. 2008; 130:11282–11283. [PubMed: 18680251]
36. Marassi FM, Gesell JJ, Valente AP, Kim Y, Oblatt-Montal M, Montal M, Opella SJ. Dilute Spin-Exchange Assignment of Solid-State Nmr Spectra of Oriented Proteins: Acetylcholine M2 in Bilayers. J Biomol NMR. 1999; 14:141–148. [PubMed: 10427741]
37. Traaseth NJ, Gopinath T, Veglia G. On the Performance of Spin Diffusion Nmr Techniques in Oriented Solids: Prospects for Resonance Assignments and Distance Measurements from Separated Local Field Experiments. J Phys Chem B. 2010; 114:13872–13880. [PubMed: 20936833]
38. Pines A, Shattuck TW. Carbon-13 Proton Nmr Cross-Polarization Times in Solid Adamantane. J Chem Phys. 1974; 61:1255–1256.
39. Lee JS, Khitrin AK. Adiabatic Cross-Polarization Via Intermediate Dipolar-Ordered State. J Magn Reson. 2005; 177:152–154. [PubMed: 16084118]
40. Lobo NP, Ramanathan KV. Sensitivity Enhancement in Solid-State Separated Local Field Nmr Experiments by the Use of Adiabatic Cross-Polarization. J Phys Chem Letters. 2011; 2:1183–1188.
41. Khitrin AK, Xu J, Ramamoorthy A. Cross-Correlations between Low-Gamma Nuclei in Solids Via a Common Dipolar Bath. J Magn Reson. 2011; 212:95–101. [PubMed: 21820340]
42. Hartmann SR, Hahn EL. Nuclear Double Resonance in the Rotating Frame. Physical Review. 1962; 128:2042–2053.
43. Lee M, Goldburg WI. Nuclear-Magnetic-Resonance Line Narrowing by a Rotating Rf Field. Physical Review. 1965; 140:A1261–A1271.

44. Pines A, Gibby MG, Waugh JS. Proton-Enhanced Nuclear Induction Spectroscopy. A Method for High Resolution Nmr of Dilute Spins in Solids. J Chem Phys. 1972; 56:1776–1777.
45. Dvinskikh SV, Zimmermann H, Maliniak A, Sandström D. Heteronuclear Dipolar Recoupling in Solid-State Nuclear Magnetic Resonance by Amplitude-, Phase-, and Frequency-Modulated Lee-Goldburg Cross-Polarization. J Chem Phys. 2005; 122:44512. [PubMed: 15740272]
46. Schanda P, Meier BH, Ernst M. Accurate Measurement of One-Bond H–X Heteronuclear Dipolar Couplings in Mas Solid-State Nmr. J Magn Reson. 2011; 210:246–259. [PubMed: 21482161]
47. Zhang R, Chen Y, Chen T, Sun P, Li B, Ding D. Accessing Structure and Dynamics of Mobile Phase in Organic Solids by Real-Time T1c Filter Pisema Nmr Spectroscopy. J Phys Chem A. 2012; 116:979–984. [PubMed: 22185485]
48. Lorieau JL, Day LA, McDermott AE. Conformational Dynamics of an Intact Virus: Order Parameters for the Coat Protein of Pf1 Bacteriophage. Proc Natl Acad Sci U S A. 2008; 105:10366–10371. [PubMed: 18653759]
49. Wu CH, Das BB, Opella SJ. (1)H-(13)C Hetero-Nuclear Dipole-Dipole Couplings of Methyl Groups in Stationary and Magic Angle Spinning Solid-State Nmr Experiments of Peptides Proteins. J Magn Reson. 2010; 202:127–134. [PubMed: 19896874]
50. Levitt, MH.; Grant, DM.; Harris, RK. Symmetry-Based Pulse Sequences in Magic-Angle Spinning Solid-State Nmr. In: McDermott, AE.; Polenova, T., editors. Solid State Nmr Studies of Biopolymers. John Wiley & Sons; 2012. p. 229
51. Zhao X, Hoffbauer W, Schmedt auf der Günne J, Levitt MH. Heteronuclear Polarization Transfer by Symmetry-Based Recoupling Sequences in Solid-State Nmr. Solid State Nucl Magn Reson. 2004; 26:57–64. [PubMed: 15276635]
52. Hou G, Byeon IJ, Ahn J, Gronenborn AM, Polenova T. 1h-13c/1h-15n Heteronuclear Dipolar Recoupling by R-Symmetry Sequences under Fast Magic Angle Spinning for Dynamics Analysis of Biological and Organic Solids. J Am Chem Soc. 2011; 133:18646–18655. [PubMed: 21995349]
53. Schmidt-Rohr K, Nanz D, Emsley L, Pines A. Nmr Measurement of Resolved Heteronuclear Dipole Couplings in Liquid Crystals and Lipids. J Phys Chem. 1994; 98:6668–6670.
54. Petkova AT, Baldus M, Belenky M, Hong M, Griffin RG, Herzfeld J. Backbone and Side Chain Assignment Strategies for Multiply Labeled Membrane Peptides and Proteins in the Solid State. J Magn Reson. 2003; 160:1–12. [PubMed: 12565042]

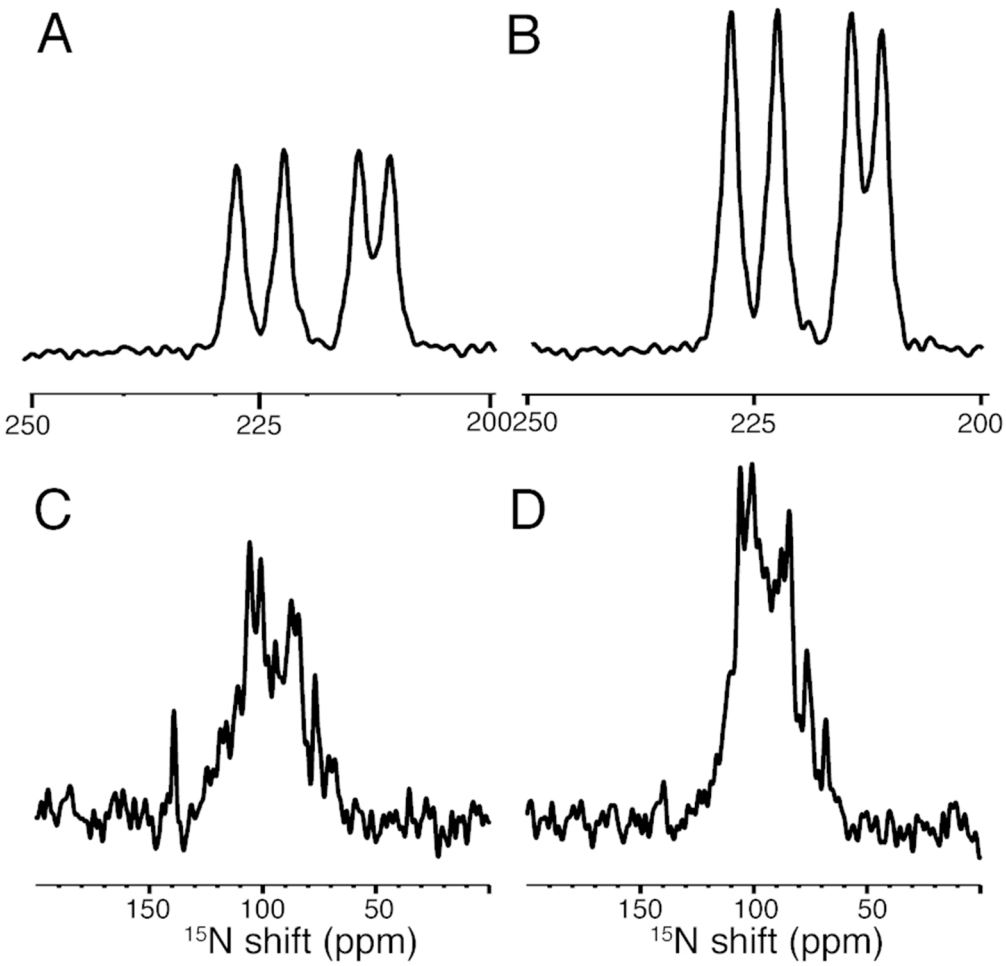

Figure 1.

^{15}N NMR spectra of a peptide crystal and a protein obtained by different methods of cross-polarization. A. Spectrum of a single crystal of ^{15}N-Acetyl Leucine (NAL) at an arbitrary orientation obtained using CP-MOIST. B. Same as in Panel A, except that the spectrum was obtained using CP-ADRF. C. CP-MOIST spectrum of uniformly ^{15}N labeled Pf1 coat protein in a magnetically aligned unflipped q=3.2 DMPC/DHPC bicelles with the bilayer normal perpendicular to the direction of the magnetic field. D. CP-ADRF spectrum of Pf1 bicelle sample. All spectra were obtained for cross-polarization contact periods between 1ms (A, C and D) and 3 ms for B. All of the spectra were obtained on a Bruker Avance spectrometer with a ^{1}H resonance frequency of 700 MHz using a home-built double-resonance probe. 50 kHz RF amplitude SPINAL modulated decoupling was applied during data acquisition. Spectra were recorded at room temperature for single crystal and 42 ºC for a bicelle sample.

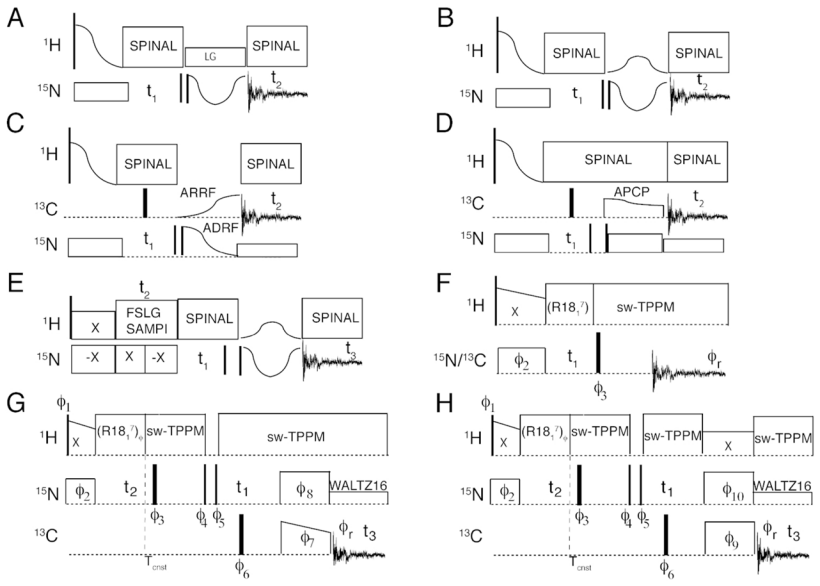

Figure 2.

Timing diagrams for two- and three- dimensional correlation experiments on stationary and magic angle sample spinning. A. and B. ^{15}N detected homonuclear correlation spectroscopy with ADRF-CP and adiabatic mixing with demagnetization-remagnetization of ^{15}N nuclei in static oriented samples. C. and D. ADRF-CP and adiabatic passage CP (APCP) in ^{13}C detected $^{13}C/^{15}N$ two-dimensional correlation in oriented samples respectively. E. Three-dimensional separated local field spectroscopy correlating ^{1}H-$^{15}N/^{15}N/^{15}N$ frequencies. Half-Gauss line shapes with amplitude modulation are used for demagnetization and remagnetization. G. and H. ^{13}C detected three-dimensional separated local field spectroscopy for magic angle spinning experiments correlating ^{1}H-^{15}N dipolar coupling with $^{15}N/^{13}C$ shift correlation. G, Adiabatic passage CP mixing under spectrally induced filtering in combination with cross-polarization (SPECIFIC-CP). H, Proton assisted insensitive nuclei CP (PAIN-CP) mixing. Thin and wider dark lines represent the hard 90º and 180º pulses. Rectangular boxes represent either continuous wave or SPINAL modulated RF pulses. Tangential line shapes are used for adiabatic passage cross polarization (APCP). The phase cycling for G and H are as follows; ϕ_1= 1 3, ϕ_2= 0 0 2 2, ϕ_3= 1 1 3 3, ϕ_4= 3, ϕ_5= 1, ϕ_6= 8(0), ϕ_7= 4(0) 4(2), ϕ_8= 4(0) 4(1) 4(2) 4(3), ϕ_9=2(0) 2(2), ϕ_{10}= 4(0) 4(2) and receivers at $\phi_{DCP}=\phi_1+\phi_7+\phi_8$ and $\phi_{PAIN}=\phi_1+\phi_9+\phi_{10}$.

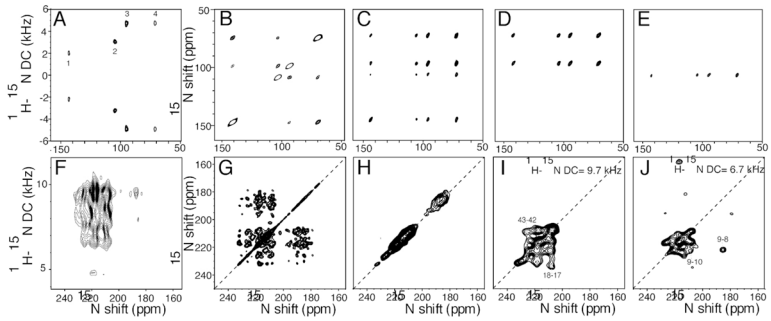

Figure 3.

Experimental two-dimensional ^{15}N-detected spectra. Top row: A, B., C., D., and E. are of a single crystal of NAL at an arbitrary orientation. Bottom row: F., G., H., I, and J. are of a magnetically aligned sample of uniformly ^{15}N labeled Pf1 bacteriophage at 0 ºC. A. SLF spectrum obtained with the SAMPI4 pulse sequence. B. ^{15}N/^{15}N correlation spectrum obtained from a 4s proton driven spin diffusion mixing time. C. Same as Panel B but obtained using the pulse scheme shown in Figure 2A and a total adiabatic mixing time of 6 ms. D. and E. are two-dimensional planes extracted from a three-dimensional spectrum at dipolar frequencies of 5 kHz and 3 kHz, respectively. F. Same as Panel A. but obtained with 2ms adiabatic mixing using the pulse scheme shown in Figure 2E and without the incorporation of ^{15}N shift evolution period (t_1). G. same as Panel C. but obtained with 2 ms mixing. H. same as G. but obtained under heteronuclear decoupling pulses applied on the ^{1}H channel and simultaneous adiabatic mixing on the ^{15}N channel. I. and J. Same as in D. and E. but extracted at dipolar frequencies of 9.7 kHz and 6.7 kHz, respectively. Resonance assignments are marked.

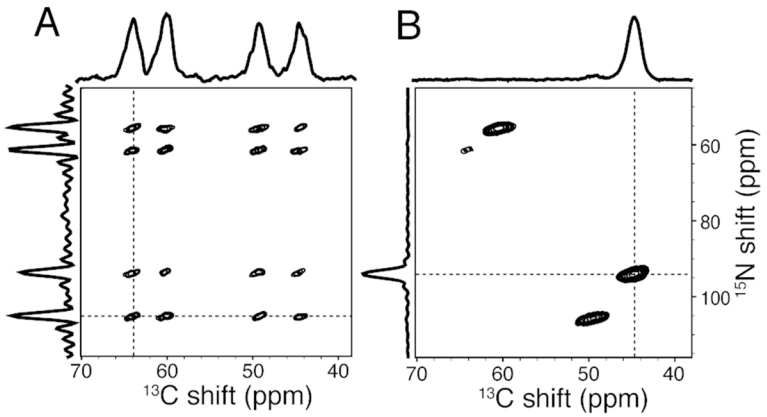

Figure 4.

^{13}C detected two-dimensional ^{13}C/^{15}N correlation spectra obtained on a single crystal of ^{13}Cα/^{15}N labeled N-Acetyl Leucine (NAL). A. NMR spectrum obtained using the pulse scheme in Figure 2C. B. Spectrum obtained using the pulse scheme in Figure 2D. One-dimensional slices taken at the frequencies marked with dotted lines are shown along the sides of the two-dimensional plots.

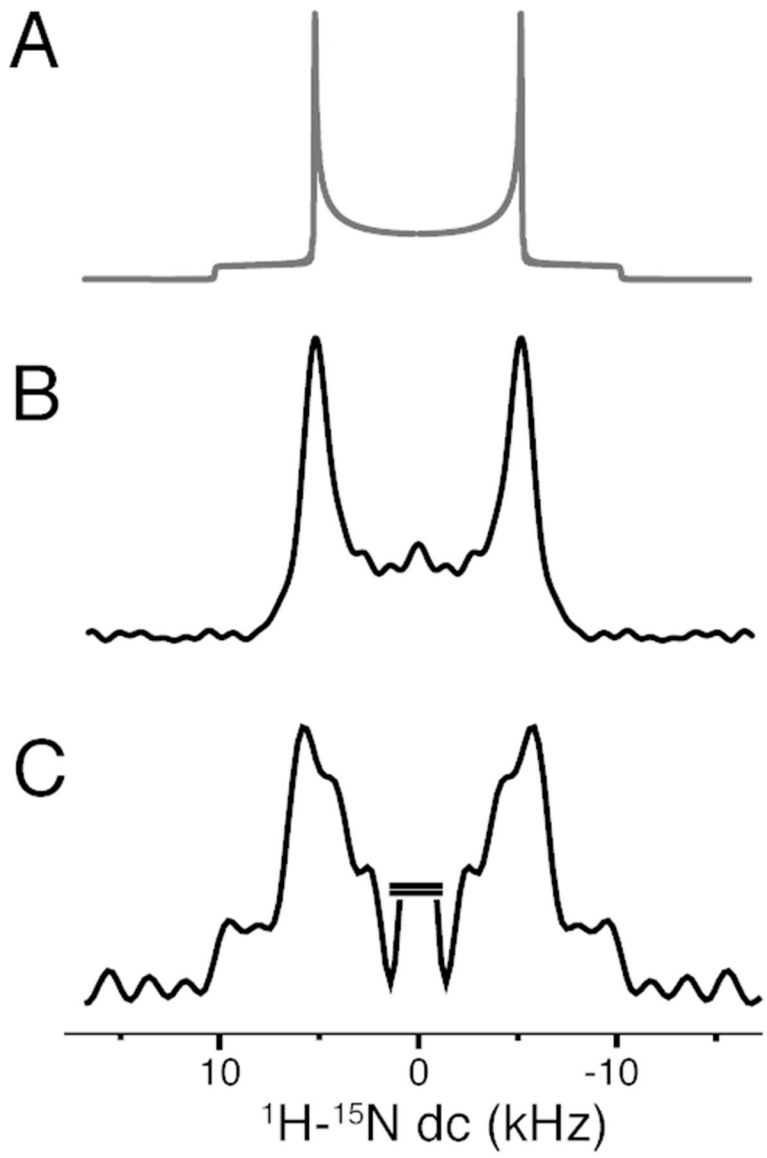

Figure 5.

One dimensional Pake doublets for ^{1}H-^{15}N dipole-dipole interactions in a poly crystalline sample of uniform ^{13}C, ^{15}N labeled NAL. A. Simulated Pake doublet for a dipolar coupling constant of 10 kHz. B. Experimental measurement of recoupled powder spectrum using $R18^{7}_{1}$ symmetry pulse scheme under 11 kHz MAS. C. Experimental, Pake doublet extracted from a SLF-2D experiment acquired using PITANSEMA under 11 kHz MAS.

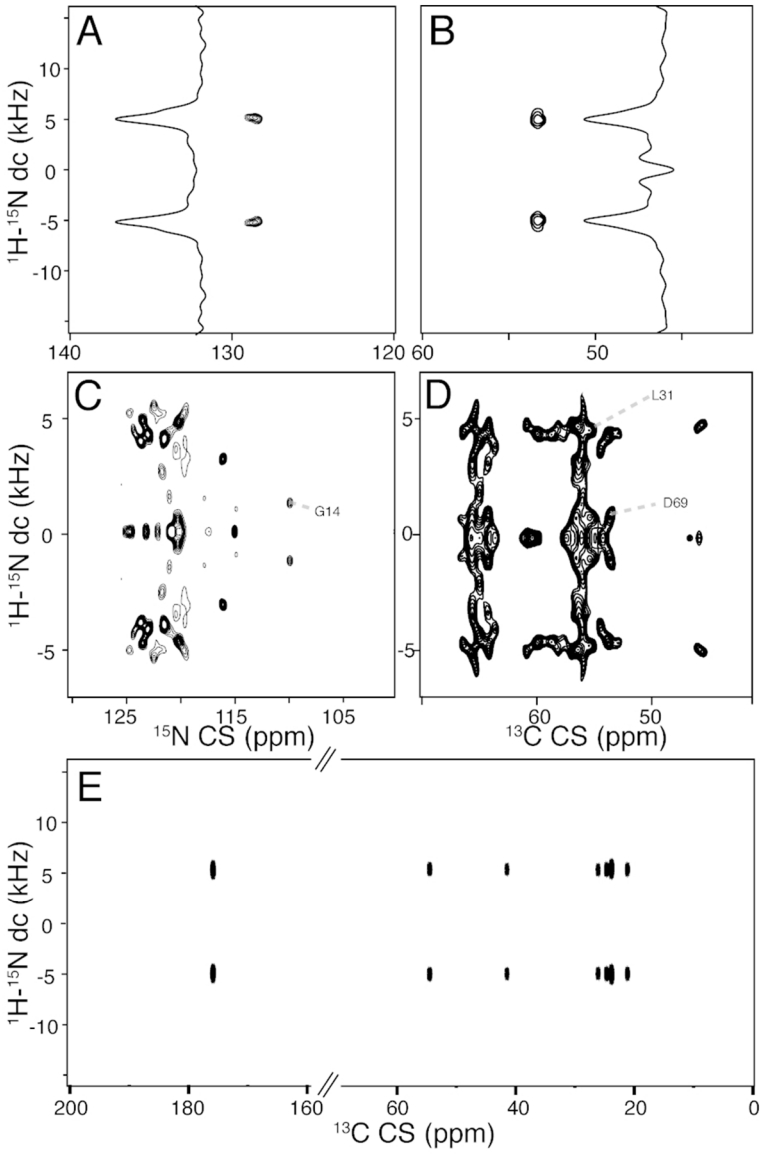

Figure 6.

Two-dimensional SLF ^{15}N and ^{13}C detected ^{1}H-^{15}N dipolar frequency measurements. Experiments were carried out using the pulse schemes shown in Figure 2F– H. A. ^{1}H-^{15}N DC/^{15}N shift correlation spectra on a single crystal sample of uniformly ^{13}C/^{15}N labeled NAL. Spectrum was recorded using the pulse scheme shown in Figure 2F. C. Same as Panel A. except for a 60 residue membrane protein, MerFt, in unoriented DMPC bilayers at 25 ºC. B. and D., same as A. and C. respectively but with ^{15}N edited ^{13}C detection. ^{1}H-^{15}N DC/^{13}Cα spectra were recorded using the pulse scheme shown in Figure 2G without the ^{15}N shift evolution. E., same as Panel B. but acquired under PAIN-CP mixing using the pulse scheme shown in Figure 2H. Note that the full dipolar spectrum is scaled to show the perpendicular edges of the dipolar Pake pattern. 11 kHz MAS with 4s recycle delay was used to obtain the two-dimensional spectra.

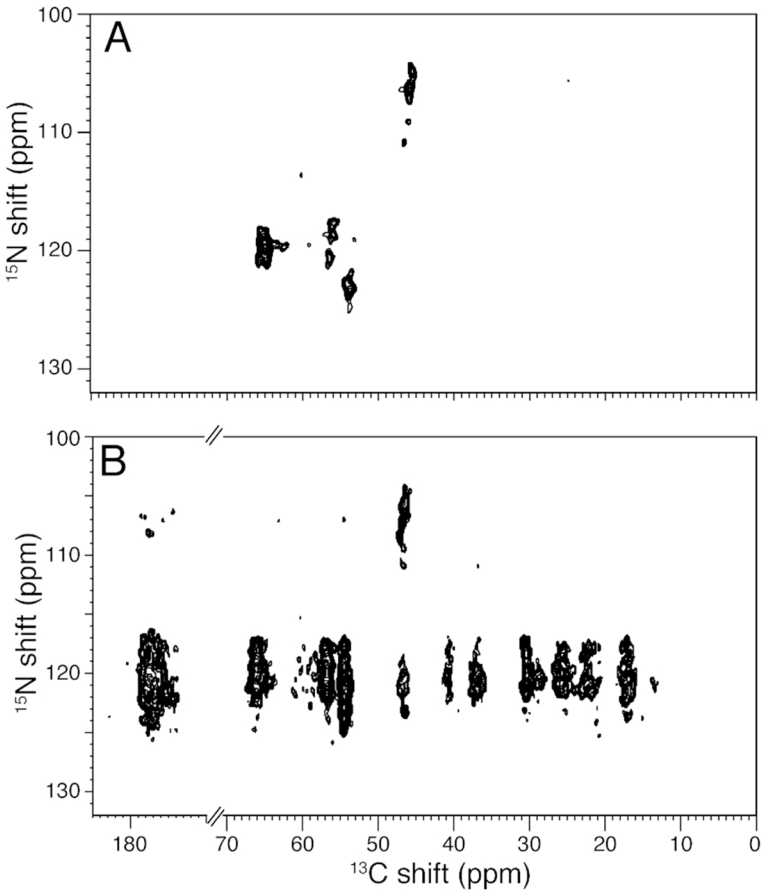

Figure 7.

^{13}C detected two-dimensional ^{13}C/^{15}N correlation spectra obtained on a uniform ^{13}Cα/^{15}N labeled Pf1 coat protein in DMPC bilayer. A. SPECIFIC CP mixing. B. PAIN-CP mixing. Both spectra were recorded at 25 ºC and 11 kHz MAS. 3.6 and 1.8 ms ^{13}C/^{15}N mixing periods were used to record spectra A. and B. respectively.

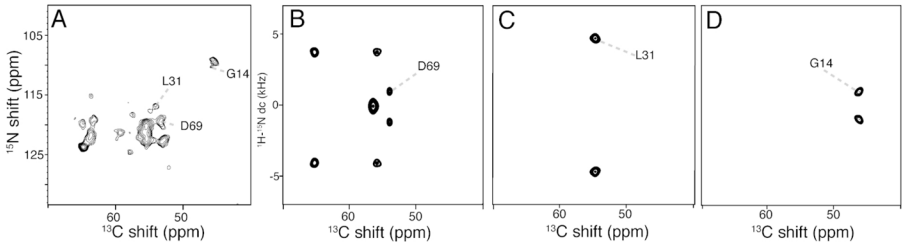

Figure 8.

Two-dimensional planes from a three-dimensional SLF experiment correlating ^{1}H-^{15}N DC/^{15}N/^{13}C shifts. The experiment was carried out using the pulse scheme shown in Figure 2G. A. First ^{15}N/^{13}Cα correlation spectrum. B., C., and D. Planes correlating ^{1}H-^{15}N DC/^{13}Cα shifts at various ^{15}N shifts. 12 ms, 6 ms and 5 ms evolution periods were used to obtain the ^{13}C, ^{15}N shifts and ^{1}H-^{15}N dipolar coupling. Equal numbers of data points were linear predicted for the domains yielding the ^{15}N shifts.